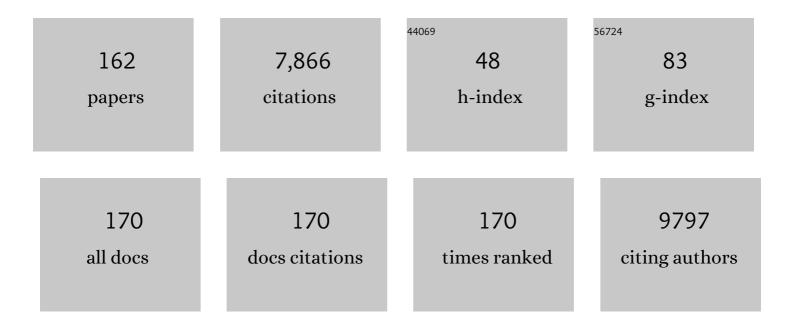
List of Publications by Year in descending order

Source: https://exaly.com/author-pdf/1314629/publications.pdf Version: 2024-02-01



#	Article	IF	CITATIONS
1	Photo-mechanical effects in azobenzene-containing soft materials. Soft Matter, 2007, 3, 1249.	2.7	512
2	Novel photo-switching using azobenzene functional materials. Journal of Photochemistry and Photobiology A: Chemistry, 2006, 182, 250-261.	3.9	485
3	Azobenzene photomechanics: prospects and potential applications. Polymer Bulletin, 2012, 69, 967-1006.	3.3	339
4	Diamond family of nanoparticle superlattices. Science, 2016, 351, 582-586.	12.6	331
5	A general strategy for the DNA-mediated self-assembly of functional nanoparticles into heterogeneous systems. Nature Nanotechnology, 2013, 8, 865-872.	31.5	267
6	All-optical patterning of azo polymer films. Current Opinion in Solid State and Materials Science, 2001, 5, 487-494.	11.5	213
7	Superlattices assembled through shape-induced directional binding. Nature Communications, 2015, 6, 6912.	12.8	188
8	Effect of Confinement on Structure, Water Solubility, and Water Transport in Nafion Thin Films. Macromolecules, 2012, 45, 7920-7930.	4.8	172
9	Ordered three-dimensional nanomaterials using DNA-prescribed and valence-controlled material voxels. Nature Materials, 2020, 19, 789-796.	27.5	172
10	Dynamic Thermal Field-Induced Gradient Soft-Shear for Highly Oriented Block Copolymer Thin Films. ACS Nano, 2012, 6, 10335-10342.	14.6	124
11	Epitaxial Growth of Molecular Crystals on van der Waals Substrates for Highâ€Performance Organic Electronics. Advanced Materials, 2014, 26, 2812-2817.	21.0	120
12	Cooperative Ordering and Kinetics of Cellulose Nanocrystal Alignment in a Magnetic Field. Langmuir, 2016, 32, 7564-7571.	3.5	119
13	Nanoimprint-Induced Molecular Orientation in Semiconducting Polymer Nanostructures. ACS Nano, 2011, 5, 7532-7538.	14.6	117
14	Arbitrary lattice symmetries via block copolymer nanomeshes. Nature Communications, 2015, 6, 7448.	12.8	116
15	Millisecond Ordering of Block Copolymer Films <i>via</i> Photothermal Gradients. ACS Nano, 2015, 9, 3896-3906.	14.6	112
16	Interparticle Spacing and Structural Ordering in Superlattice PbS Nanocrystal Solids Undergoing Ligand Exchange. Chemistry of Materials, 2015, 27, 474-482.	6.7	111
17	Injectable Anisotropic Nanocomposite Hydrogels Direct in Situ Growth and Alignment of Myotubes. Nano Letters, 2017, 17, 6487-6495.	9.1	111
18	Photomechanical Surface Patterning in Azo-Polymer Materials. Macromolecules, 2006, 39, 9320-9326.	4.8	107

#	Article	IF	CITATIONS
19	Photomechanical Effects in Azo-Polymers Studied by Neutron Reflectometry. Macromolecules, 2006, 39, 9311-9319.	4.8	92
20	Challenges in Fabrication of Mesoporous Carbon Films with Ordered Cylindrical Pores <i>via</i> Phenolic Oligomer Self-Assembly with Triblock Copolymers. ACS Nano, 2010, 4, 189-198.	14.6	90
21	Temperature modeling of laser-irradiated azo-polymer thin films. Journal of Chemical Physics, 2004, 120, 1089-1096.	3.0	89
22	<i>Xi-cam</i> : a versatile interface for data visualization and analysis. Journal of Synchrotron Radiation, 2018, 25, 1261-1270.	2.4	89
23	Surface Morphology Diagram for Cylinder-Forming Block Copolymer Thin Films. ACS Nano, 2008, 2, 2331-2341.	14.6	82
24	A Supramolecular Complex in Smallâ€Molecule Solar Cells based on Contorted Aromatic Molecules. Angewandte Chemie - International Edition, 2012, 51, 8594-8597.	13.8	82
25	Rapid ordering of block copolymer thin films. Journal of Physics Condensed Matter, 2016, 28, 403002.	1.8	80
26	Aberration-Corrected Electron Beam Lithography at the One Nanometer Length Scale. Nano Letters, 2017, 17, 4562-4567.	9.1	80
27	Tuning Molecular Relaxation for Vertical Orientation in Cylindrical Block Copolymer Films via Sharp Dynamic Zone Annealing. Macromolecules, 2012, 45, 7107-7117.	4.8	78
28	Non-native three-dimensional block copolymer morphologies. Nature Communications, 2016, 7, 13988.	12.8	77
29	Two-Dimensional DNA-Programmable Assembly of Nanoparticles at Liquid Interfaces. Journal of the American Chemical Society, 2014, 136, 8323-8332.	13.7	73
30	Anomalously Large Polarization Effect Responsible for Excitonic Red Shifts in PbSe Quantum Dot Solids. Journal of Physical Chemistry Letters, 2011, 2, 795-800.	4.6	72
31	Linear Mesostructures in DNA–Nanorod Self-Assembly. ACS Nano, 2013, 7, 5437-5445.	14.6	72
32	A Kriging-Based Approach to Autonomous Experimentation with Applications to X-Ray Scattering. Scientific Reports, 2019, 9, 11809.	3.3	72
33	Evolution of block-copolymer order through a moving thermal zone. Soft Matter, 2010, 6, 92-99.	2.7	65
34	Directed Self-Assembly of Block Copolymers for High Breakdown Strength Polymer Film Capacitors. ACS Applied Materials & Interfaces, 2016, 8, 7966-7976.	8.0	65
35	Beyond native block copolymer morphologies. Molecular Systems Design and Engineering, 2017, 2, 518-538.	3.4	62
36	Robust conductive mesoporous carbon–silica composite films with highly ordered and oriented orthorhombic structures from triblock-copolymer template co-assembly. Journal of Materials Chemistry, 2010, 20, 1691.	6.7	55

#	Article	IF	CITATIONS
37	Large-Scale Roll-to-Roll Fabrication of Vertically Oriented Block Copolymer Thin Films. ACS Nano, 2013, 7, 5291-5299.	14.6	55
38	Air–Liquid Interfacial Self-Assembly of Conjugated Block Copolymers into Ordered Nanowire Arrays. ACS Nano, 2014, 8, 12755-12762.	14.6	55
39	Templated Self-Assembly of a PS- <i>Branch</i> -PDMS Bottlebrush Copolymer. Nano Letters, 2018, 18, 4360-4369.	9.1	54
40	Complementary Hydrogen Bonding and Block Copolymer Self-Assembly in Cooperation toward Stable Solar Cells with Tunable Morphologies. Macromolecules, 2013, 46, 9021-9031.	4.8	53
41	Nanostructured Surfaces Frustrate Polymer Semiconductor Molecular Orientation. ACS Nano, 2014, 8, 243-249.	14.6	53
42	Stable and Controllable Polymer/Fullerene Composite Nanofibers through Cooperative Noncovalent Interactions for Organic Photovoltaics. Chemistry of Materials, 2014, 26, 3747-3756.	6.7	51
43	Magnetic Alignment of Block Copolymer Microdomains by Intrinsic Chain Anisotropy. Physical Review Letters, 2015, 115, 258302.	7.8	51
44	Highly Crystalline Films of PCPDTBT with Branched Side Chains by Solvent Vapor Crystallization: Influence on Optoâ€Electronic Properties. Advanced Materials, 2015, 27, 1223-1228.	21.0	51
45	Selective directed self-assembly of coexisting morphologies using block copolymer blends. Nature Communications, 2016, 7, 12366.	12.8	51
46	Water Distribution in Multilayers of Weak Polyelectrolytes. Langmuir, 2006, 22, 5137-5143.	3.5	50
47	Unusual packing of soft-shelled nanocubes. Science Advances, 2019, 5, eaaw2399.	10.3	50
48	Latent Alignment in Pathway-Dependent Ordering of Block Copolymer Thin Films. Nano Letters, 2015, 15, 5221-5228.	9.1	49
49	Solvent Retention in Thin Spin-Coated Polystyrene and Poly(methyl methacrylate) Homopolymer Films Studied By Neutron Reflectometry. Macromolecules, 2010, 43, 1117-1123.	4.8	48
50	Quaternary Organic Solar Cells Enhanced by Cocrystalline Squaraines with Power Conversion Efficiencies >10%. Advanced Energy Materials, 2016, 6, 1600660.	19.5	46
51	Reordering transitions during annealing of block copolymer cylinder phases. Soft Matter, 2016, 12, 281-294.	2.7	46
52	Grazing-incidence transmission X-ray scattering: surface scattering in the Born approximation. Journal of Applied Crystallography, 2013, 46, 165-172.	4.5	45
53	Periodic lattices of arbitrary nano-objects: modeling and applications for self-assembled systems. Journal of Applied Crystallography, 2014, 47, 118-129.	4.5	45
54	<i>In Situ</i> Characterization of the Self-Assembly of a Polystyrene–Polydimethylsiloxane Block Copolymer during Solvent Vapor Annealing. Macromolecules, 2015, 48, 8574-8584.	4.8	45

#	Article	IF	CITATIONS
55	Resilient three-dimensional ordered architectures assembled from nanoparticles by DNA. Science Advances, 2021, 7, .	10.3	45
56	Gaussian processes for autonomous data acquisition at large-scale synchrotron and neutron facilities. Nature Reviews Physics, 2021, 3, 685-697.	26.6	44
57	In Situ Method for Measuring the Mechanical Properties of Nafion Thin Films during Hydration Cycles. ACS Applied Materials & Interfaces, 2015, 7, 17874-17883.	8.0	43
58	Operando Grazing Incidence Small-Angle X-ray Scattering/X-ray Diffraction of Model Ordered Mesoporous Lithium-Ion Battery Anodes. ACS Nano, 2017, 11, 1443-1454.	14.6	42
59	Surface-Induced Nanostructure and Water Transport of Thin Proton-Conducting Polymer Films. Macromolecules, 2013, 46, 5630-5637.	4.8	41
60	Molecular Origin of Photovoltaic Performance in Donor- <i>block</i> -Acceptor All-Conjugated Block Copolymers. Macromolecules, 2015, 48, 8346-8353.	4.8	41
61	Rapid Ordering in "Wet Brush―Block Copolymer/Homopolymer Ternary Blends. ACS Nano, 2017, 11, 12326-12336.	14.6	40
62	Lamellar and liquid crystal ordering in solvent-annealed all-conjugated block copolymers. Soft Matter, 2014, 10, 3817-3825.	2.7	39
63	Self-Assembled Phases of Block Copolymer Blend Thin Films. ACS Nano, 2014, 8, 10582-10588.	14.6	39
64	Linking Group Influences Charge Separation and Recombination in Allâ€Conjugated Block Copolymer Photovoltaics. Advanced Functional Materials, 2015, 25, 5578-5585.	14.9	38
65	Autonomous materials discovery driven by Gaussian process regression with inhomogeneous measurement noise and anisotropic kernels. Scientific Reports, 2020, 10, 17663.	3.3	38
66	Molecular Dynamics Study of the Role of the Free Surface on Block Copolymer Thin Film Morphology and Alignment. ACS Nano, 2011, 5, 2895-2907.	14.6	36
67	One-Volt Operation of High-Current Vertical Channel Polymer Semiconductor Field-Effect Transistors. Nano Letters, 2012, 12, 4181-4186.	9.1	36
68	Disordered nanoparticle interfaces for directed self-assembly. Soft Matter, 2009, 5, 622-628.	2.7	35
69	Block Copolymer Response to Photothermal Stress Fields. Macromolecules, 2015, 48, 4591-4598.	4.8	34
70	Ordering Pathway of Block Copolymers under Dynamic Thermal Gradients Studied by <i>in Situ</i> GISAXS. Macromolecules, 2016, 49, 8633-8642.	4.8	34
71	Inverse Temperature Dependence of Charge Carrier Hopping in Quantum Dot Solids. ACS Nano, 2018, 12, 7741-7749.	14.6	33
72	Ion distribution in multilayers of weak polyelectrolytes: A neutron reflectometry study. Journal of Chemical Physics, 2008, 129, 084901.	3.0	32

#	Article	IF	CITATIONS
73	Nano-structuring polymer/fullerene composites through the interplay of conjugated polymer crystallization, block copolymer self-assembly and complementary hydrogen bonding interactions. Polymer Chemistry, 2015, 6, 721-731.	3.9	30
74	Thickness-dependence of block copolymer coarsening kinetics. Soft Matter, 2017, 13, 3275-3283.	2.7	29
75	Thickness-Dependent Ordering Kinetics in Cylindrical Block Copolymer/Homopolymer Ternary Blends. Macromolecules, 2018, 51, 10259-10270.	4.8	29
76	Direct Observation of Micelle Fragmentation via In Situ Liquid-Phase Transmission Electron Microscopy. ACS Macro Letters, 2020, 9, 756-761.	4.8	29
77	Pathway-engineering for highly-aligned block copolymer arrays. Nanoscale, 2018, 10, 416-427.	5.6	28
78	Advances in Kriging-Based Autonomous X-Ray Scattering Experiments. Scientific Reports, 2020, 10, 1325.	3.3	28
79	Confinement of surface patterning in azo-polymer thin films. Journal of Chemical Physics, 2007, 126, 094908.	3.0	27
80	Enhanced charge collection in confined bulk heterojunction organic solar cells. Applied Physics Letters, 2011, 99, 163301.	3.3	27
81	Variable temperature, relative humidity (0%–100%), and liquid neutron reflectometry sample cell suitable for polymeric and biomimetic materials. Review of Scientific Instruments, 2005, 76, 065101.	1.3	26
82	Network-Stabilized Bulk Heterojunction Organic Photovoltaics. Chemistry of Materials, 2018, 30, 8314-8321.	6.7	26
83	Thin Film Self-Assembly of a Silicon-Containing Rod–Coil Liquid Crystalline Block Copolymer. Macromolecules, 2019, 52, 679-689.	4.8	26
84	Thermally-induced transition of lamellae orientation in block-copolymer films on â€~neutral' nanoparticle-coated substrates. Soft Matter, 2015, 11, 5154-5167.	2.7	25
85	Wet Brush Homopolymers as "Smart Solvents―for Rapid, Large Period Block Copolymer Thin Film Self-Assembly. Macromolecules, 2020, 53, 1098-1113.	4.8	24
86	Stable Thermotropic 3D and 2D Double Gyroid Nanostructures with Subâ€2â€nm Feature Size from Scalable Sugar–Polyolefin Conjugates. Angewandte Chemie - International Edition, 2021, 60, 8710-8716.	13.8	24
87	Molecular Orientation and Performance of Nanoimprinted Polymer-Based Blend Thin Film Solar Cells. Chemistry of Materials, 2015, 27, 60-66.	6.7	23
88	X-Ray Scattering Image Classification Using Deep Learning. , 2017, , .		23
89	Double-Layer Morphologies from a Silicon-Containing ABA Triblock Copolymer. ACS Nano, 2018, 12, 6193-6202.	14.6	23
90	Instrumentation for <i>In situ/Operando</i> X-ray Scattering Studies of Polymer Additive Manufacturing Processes. Synchrotron Radiation News, 2019, 32, 20-27.	0.8	22

#	Article	IF	CITATIONS
91	Dendrimer Ligand Directed Nanoplate Assembly. ACS Nano, 2019, 13, 14241-14251.	14.6	22
92	Target Patterns Induced by Fixed Nanoparticles in Block Copolymer Films. ACS Nano, 2009, 3, 2115-2120.	14.6	21
93	Facile control of long range orientation in mesoporous carbon films with thermal zone annealing velocity. Nanoscale, 2013, 5, 12440.	5.6	21
94	Evidence of Stratification in Binary Colloidal Films from Microbeam X-ray Scattering: Toward Optimizing the Evaporative Assembly Processes for Coatings. ACS Applied Nano Materials, 2018, 1, 4211-4217.	5.0	21
95	Sandwich layering in binary nanoparticle films and effect of size ratio on stratification behavior. Journal of Colloid and Interface Science, 2019, 538, 209-217.	9.4	20
96	Edge States Drive Exciton Dissociation in Ruddlesden–Popper Lead Halide Perovskite Thin Films. , 2020, 2, 1360-1367.		20
97	Combinatorial Block Copolymer Ordering on Tunable Rough Substrates. Macromolecules, 2012, 45, 4303-4314.	4.8	19
98	In Situ Study of ABC Triblock Terpolymer Self-Assembly under Solvent Vapor Annealing. Macromolecules, 2019, 52, 1853-1863.	4.8	19
99	Photothermally Directed Assembly of Block Copolymers. Advanced Materials Interfaces, 2020, 7, 1901679.	3.7	19
100	Through-Thickness Vertically Ordered Lamellar Block Copolymer Thin Films on Unmodified Quartz with Cold Zone Annealing. Nano Letters, 2017, 17, 7814-7823.	9.1	18
101	Self-assembly of a silicon-containing side-chain liquid crystalline block copolymer in bulk and in thin films: kinetic pathway of a cylinder to sphere transition. Nanoscale, 2019, 11, 285-293.	5.6	18
102	Implications of Grain Size Variation in Magnetic Field Alignment of Block Copolymer Blends. ACS Macro Letters, 2017, 6, 404-409.	4.8	17
103	Vertical Lamellae Formed by Two-Step Annealing of a Rod–Coil Liquid Crystalline Block Copolymer Thin Film. ACS Nano, 2020, 14, 4289-4297.	14.6	17
104	Self-assembly of single dielectric nanoparticle layers and integration in polymer-based solar cells. Applied Physics Letters, 2012, 101, 063105.	3.3	16
105	Strongly Correlated Alignment of Fluorinated 5,11â€Bis(triethylgermylethynyl)anthradithiophene Crystallites in Solutionâ€Processed Fieldâ€Effect Transistors. ChemPhysChem, 2014, 15, 2913-2916.	2.1	16
106	Mesoporous Carbon–Vanadium Oxide Films by Resol-Assisted, Triblock Copolymer-Templated Cooperative Self-Assembly. ACS Applied Materials & Interfaces, 2014, 6, 19288-19298.	8.0	15
107	X-Ray scattering and physicochemical studies of trialkylamine/carboxylic acid mixtures: nanoscale structure in pseudoprotic ionic liquids and related solutions. Physical Chemistry Chemical Physics, 2018, 20, 18639-18646.	2.8	15
108	Strain rate dependent nanostructure of hydrogels with reversible hydrophobic associations during uniaxial extension. Soft Matter, 2019, 15, 227-236.	2.7	15

#	Article	IF	CITATIONS
109	Electrospray deposition tool: Creating compositionally gradient libraries of nanomaterials. Review of Scientific Instruments, 2020, 91, 013701.	1.3	15
110	Experiments and Simulations Probing Local Domain Bulge and String Assembly of Aligned Nanoplates in a Lamellar Diblock Copolymer. Macromolecules, 2019, 52, 8989-8999.	4.8	14
111	Thermally Reversible Surface Morphology Transition in Thin Diblock Copolymer Films. ACS Nano, 2010, 4, 3653-3660.	14.6	13
112	Reticulated Organic Photovoltaics. Advanced Functional Materials, 2012, 22, 1167-1173.	14.9	13
113	Molecular Weight Dependence of Block Copolymer Micelle Fragmentation Kinetics. Journal of the American Chemical Society, 2021, 143, 7748-7758.	13.7	13
114	Unwarping GISAXS data. IUCrJ, 2018, 5, 737-752.	2.2	13
115	Conjugated block copolymers via functionalized initiators and click chemistry. Journal of Polymer Science Part A, 2014, 52, 154-163.	2.3	12
116	Thickness Limit for Alignment of Block Copolymer Films Using Solvent Vapor Annealing with Shear. Macromolecules, 2018, 51, 4213-4219.	4.8	12
117	Film Thickness and Composition Effects in Symmetric Ternary Block Copolymer/Homopolymer Blend Films: Domain Spacing and Orientation. Macromolecules, 2021, 54, 7970-7986.	4.8	12
118	Metrics of graininess: robust quantification of grain count from the non-uniformity of scattering rings. Journal of Applied Crystallography, 2014, 47, 1855-1865.	4.5	11
119	Materials discovery: Fine-grained classification of X-ray scattering images. , 2014, , .		11
120	Aligned Morphologies in Near-Edge Regions of Block Copolymer Thin Films. Macromolecules, 2019, 52, 7224-7233.	4.8	11
121	Wiki ware could harness the Internet for science. Nature, 2006, 440, 278-278.	27.8	10
122	Control of all onjugated block copolymer crystallization via thermal and solvent annealing. Journal of Polymer Science, Part B: Polymer Physics, 2014, 52, 900-906.	2.1	10
123	Self-Organization of Quantum Rods Induced by Lipid Membrane Corrugations. Langmuir, 2015, 31, 12148-12154.	3.5	10
124	Temperature-controlled neutron reflectometry sample cell suitable for study of photoactive thin films. Review of Scientific Instruments, 2006, 77, 045106.	1.3	9
125	Chapter 17. Azobenzene Polymers as Photomechanical and Multifunctional Smart Materials. , 2007, , 424-446.		9
126	High-throughput morphology mapping of self-assembling ternary polymer blends. RSC Advances, 2020, 10, 42529-42541.	3.6	9

#	Article	IF	CITATIONS
127	Healing X-ray scattering images. IUCrJ, 2017, 4, 455-465.	2.2	9
128	X-ray scattering as a liquid and solid phase probe of ordering within sub-monolayers of iron oxide nanoparticles fabricated by electrophoretic deposition. Nanoscale, 2014, 6, 4047.	5.6	8
129	Improved Anisotropic Thermoelectric Behavior of Poly(3,4-ethylenedioxythiophene):Poly(styrenesulfonate) via Magnetophoresis. ACS Omega, 2018, 3, 12554-12561.	3.5	8
130	Nanoconfinement and Salt Synergistically Suppress Crystallization in Polyethylene Oxide. Macromolecules, 2020, 53, 1494-1501.	4.8	8
131	Robust X-ray angular correlations for the study of meso-structures. Journal of Applied Crystallography, 2017, 50, 805-819.	4.5	7
132	Future trends in synchrotron science at NSLS-II. Journal of Physics Condensed Matter, 2020, 32, 374008.	1.8	7
133	Stable Thermotropic 3D and 2D Double Gyroid Nanostructures with Subâ€2â€nm Feature Size from Scalable Sugar–Polyolefin Conjugates. Angewandte Chemie, 2021, 133, 8792-8798.	2.0	7
134	Suppression of target patterns in domain aligned cold-zone annealed block copolymer films with immobilized film-spanning nanoparticles. Soft Matter, 2014, 10, 3656.	2.7	6
135	Deep learning for analysing synchrotron data streams. , 2016, , .		6
136	Vertically grown nanowire crystals of dibenzotetrathienocoronene (DBTTC) on large-area graphene. RSC Advances, 2016, 6, 59582-59589.	3.6	6
137	Alignment frustration in block copolymer films with block copolymer grafted <scp>TiO<sub>2</sub></scp> nanoparticles under <scp>softâ€shear</scp> cold zone annealing. Polymers for Advanced Technologies, 2021, 32, 2052-2060.	3.2	6
138	Co-design Center for Exascale Machine Learning Technologies (ExaLearn). International Journal of High Performance Computing Applications, 2021, 35, 598-616.	3.7	6
139	Mechanisms of Interface Cleaning in Heterostructures Made from Polymerâ€Contaminated Graphene. Small, 2022, 18, e2201248.	10.0	6
140	Amorphous Azobenzene Polymers for Light-Induced Surface Patterning. , 0, , 145-175.		5
141	Rapid assessment of crystal orientation in semi-crystalline polymer films using rotational zone annealing and impact of orientation on mechanical properties. Soft Matter, 2017, 13, 7074-7084.	2.7	5
142	Interactive Visual Study of Multiple Attributes Learning Model of X-Ray Scattering Images. IEEE Transactions on Visualization and Computer Graphics, 2021, 27, 1312-1321.	4.4	5
143	Multi-Modal Synchrotron Characterization: Modern Techniques and Data Analysis. , 2020, , 39-64.		4
144	Robust and scalable deep learning for X-ray synchrotron image analysis. , 2017, , .		3

#	Article	IF	CITATIONS
145	Coherent amplification of X-ray scattering from meso-structures. IUCrJ, 2017, 4, 604-613.	2.2	3
146	In-Operando Tracking and Prediction of Transition in Material System using LSTM. , 2018, , .		3
147	MultiSciView: Multivariate Scientific X-ray Image Visual Exploration with Cross-Data Space Views. Visual Informatics, 2018, 2, 14-25.	4.4	3
148	Nanoscale viscosity of confined polyethylene oxide. Physical Review E, 2019, 100, 062503.	2.1	3
149	Multimodal Synchrotron Approach: Research Needs and Scientific Vision. Synchrotron Radiation News, 2020, 33, 44-47.	0.8	3
150	Excited-State Processes in Slow Motion: An Experiment in the Undergraduate Laboratory. Journal of Chemical Education, 2010, 87, 1252-1256.	2.3	2
151	Wide angle x-ray diffraction studies of nanocrystalline lead europium sulfide. Materials Letters, 2012, 89, 198-201.	2.6	2
152	Implementing nanometer-scale confinement in organic semiconductor bulk heterojunction solar cells. Journal of Photonics for Energy, 2012, 2, 021008.	1.3	2
153	Diffusion-based clustering analysis of coherent X-ray scattering patterns of self-assembled nanoparticles. , 2014, , .		2
154	Each co-author should sign to reduce risk of fraud. Nature, 2007, 450, 610-610.	27.8	1
155	A Modern Instantiation of Schillinger's Dance Notation: Choreographing with Mouse, iPad, KBow, and Kinect. Contemporary Music Review, 2011, 30, 179-186.	0.3	1
156	Solar Cells: Quaternary Organic Solar Cells Enhanced by Cocrystalline Squaraines with Power Conversion Efficiencies >10% (Adv. Energy Mater. 21/2016). Advanced Energy Materials, 2016, 6, .	19.5	1
157	Application of Analysis on the Wire to Streaming NSLS-II Beamline Data. , 2018, , .		1
158	Thin films of light-responsive polymers for sensing and surface patterning. , 2003, , .		0
159	Photo-Mechanical Azo Polymers for Light-Powered Actuation and Artificial Muscles. , 2012, , 107-151.		0
160	Addressing fundamental architectural challenges of an activity-based intelligence and advanced analytics (ABIAA) system. Proceedings of SPIE, 2015, , .	0.8	0
161	Laser-directed self-assembly of block copolymers investigated with synchrotron GISAXS. Acta Crystallographica Section A: Foundations and Advances, 2017, 73, a82-a82.	0.1	Ο

Visual Analytics for Scientific Data in NSLS-II. , 2020, , 159-168.